

Outage Performance of 3D Mobile UAV Caching for Hybrid Satellite-Terrestrial Networks

Pankaj K. Sharma, Deepika Gupta, and Dong In Kim

Abstract

In this paper, we consider a hybrid satellite-terrestrial network (HSTN) where a multiantenna satellite communicates with a ground user equipment (UE) with the help of multiple cache-enabled amplify-and-forward (AF) three-dimensional (3D) mobile unmanned aerial vehicle (UAV) relays. Herein, we employ the two fundamental most popular content (MPC) and uniform content (UC) caching schemes for two types of mobile UAV relays, namely fully 3D and fixed height. Taking into account the multiantenna satellite links and the random 3D distances between UAV relays and UE, we analyze the outage probability (OP) of considered system with MPC and UC caching schemes. We further carry out the corresponding asymptotic OP analysis to present the insights on achievable performance gains of two schemes for both types of 3D mobile UAV relaying. Specifically, we show the following: (a) MPC caching dominates the UC and no caching schemes; (b) fully 3D mobile UAV relaying outperforms its fixed height counterpart. We finally corroborate the theoretic analysis by simulations.

Index Terms

satellite communications, unmanned aerial vehicle (UAV), mobile relaying, wireless caching, outage probability.

I. INTRODUCTION

Hybrid satellite-terrestrial networks (HSTNs) with integrated terrestrial cooperative communications can effectively mitigate the impact of deleterious masking effect in satellite links and thus, are among the promising candidates for next-generation wireless systems [1], [2]. As a

Pankaj K. Sharma is with the Department of Electronics and Communication Engineering, National Institute of Technology Rourkela, Rourkela 769008, India. Email: sharmap@nitrkl.ac.in.

Deepika Gupta is with the Department of Electronics and Communication Engineering, Dr S P M International Institute of Information Technology, Naya Raipur, Naya Raipur 493661, India. Email: deepika@iiitnr.edu.in.

Dong In Kim is with the Department of Electrical and Computer Engineering, Sungkyunkwan University, Suwon, South Korea. Email: dikim@skku.ac.kr.

result, a handful of works have investigated the performance of general HSTNs by incorporating the fundamental amplify-and-forward (AF)/decode-and-forward (DF) relaying techniques [3]-[6]. Also, some works have recently investigated the performance of cognitive HSTNs [7], [8]. In majority of these HSTNs, the satellite and terrestrial link channels are modeled as Shadowed-Rician (SR) and Nakagami- m distributed. Despite of substantial efforts made towards improving the performance of HSTNs, these are inevitably affected by the intrinsic issues, namely bandwidth scarcity and latency [3], [7].

Recently, wireless caching [9] has been emerged as an effective paradigm where some popular contents are prefetched locally by the network nodes (e.g., relay, etc.) in their installed storage during off-peak hours. Such contents can be directly fetched at destination through the caching relay node in one hop which alleviates the need of its transmission from source in two hops. It reduces the overall transmission time from source-to-destination by half to tackle the intrinsic spectral efficiency and latency issues. There are two fundamental caching schemes proposed in literature [9], namely most popular content (MPC) caching and uniform content (UC) caching. While the MPC caching achieves the largest cooperative diversity gain, the UC caching achieves the largest content diversity gain. Specifically, in the MPC caching scheme, the frequently-demanded (i.e., most popular) content by the user is cached at each network node. Therefore, a cached content can be provided by one of the opportunistically selected network nodes to the user resulting in a cooperative diversity gain without any content diversity. Unlike the MPC caching, in the UC caching, each network node caches different contents uniformly from the available catalogue of data. As a result, the largest content diversity is achievable in the UC caching without cooperative diversity since a unique content can be provided by at most one network node to the user. Although neither of MPC and UC are optimal, these remain fundamental caching schemes for relay networks. A few works [10], [11] have recently applied wireless caching for relay networks. In [10], the fundamental MPC and UC caching schemes were studied for AF relay networks. Different from these schemes, a hybrid caching with optimization was studied in [11]. Counting on numerous advantages, the wireless caching has also been introduced to satellite communications [12]-[14]. In [14], the MPC and UC caching schemes for HSTNs but for terrestrial Rayleigh fading.

Furthermore, the unmanned aerial vehicles (UAVs) have recently been considered as promising candidates for future wireless networks. Backed by the low cost, portability, and three-dimensional (3D) mobility features, a rotary-wing type UAV is of particular choice for 3D

mobile relaying. A plethora of recent works [15]-[18] have attempted to present stochastic UAV mobility models for the performance analysis of UAV-based wireless networks. For instance, in [15], the authors have proposed various UAV mobility models including the random walk (RW) and random waypoint (RWP). In [16], a generalized Gauss-Markov process-based UAV mobility model has been proposed for the airborne networks. Further, in [17], [18], a mixed-mobility (MM) model was proposed for 3D UAV movement process. Eventually, based on the MM model, in [19], [20] and [21], the performance of DF and AF 3D mobile relaying have been investigated for HSTNs, respectively. Note that despite of its importance, the performance of wireless caching for HSTNs with 3D mobile UAV relaying is entirely unknown even for fundamental MPC and UC schemes.

Motivated by the above, in this paper, we investigate first time the outage probability (OP) of an HSTN that comprises of a multiantenna satellite communicating with a ground user equipment (UE) via multiple cache-enabled AF 3D mobile UAV relays. We take into account two generic deployment configurations of UAV relays, namely fully 3D mobile UAV relays and fixed height 3D mobile UAV relays. Furthermore, as followed in [10], [14], we consider the popular MPC and UC schemes for the OP as well as corresponding asymptotic OP analyses to assess their cooperative diversity gains.

Notations: $\mathbb{E}[\cdot]$ represents the statistical expectation. $\|\cdot\|$ denotes the Euclidean norm. The acronyms pdf and cdf stand for probability density function $f_X(\cdot)$ and cumulative distribution function $F_X(\cdot)$ of random variable X , respectively.

II. SYSTEM DESCRIPTION

A. System Model

As shown in Fig. 1, we consider an HSTN where a satellite S equipped with N antennas communicates with a single-antenna ground UE D via M cache-enabled single-antenna 3D UAV relays U_i , $i \in \{1, \dots, M\}$. Here, at any time t , we assume that the UAVs make 3D spatial transitions based on MM¹model [17], [18]. The instantaneous altitude of a UAV U_i at time t is denoted by $h_i(t)$ whereas the spatial location is represented as $z_i(t)$. While the UAVs operate

¹The stochastic MM model may be applied to characterize the random 3D locations of UAV relays under some control mechanisms, e.g., altitude control, trajectory control, etc., when the information about their instantaneous locations is unavailable centrally. Note that the stochastic 3D mobility-based approach is helpful when 3D spatial point processes lead to a tedious analysis.

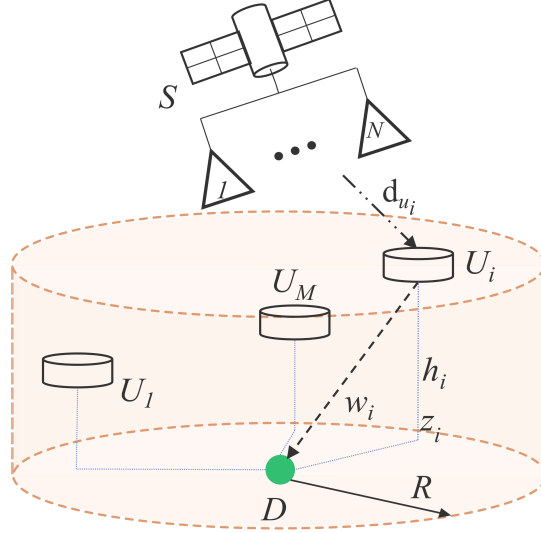


Fig. 1: HSTN system model with fully 3D mobile UAV relays.

in a 3D cylindrical space of radius R and height H ($H < R$) above the ground plane, the UE D is located at the centre of the base of this cylindrical region. Moreover, we consider that the aforementioned cylindrical region lies beneath the circular spot beam of satellite S centered around the UE D . All UAVs can update their 3D locations in discrete time slots. The channel vector from S to U_i is denoted as $\mathbf{g}_{su_i} \in \mathbb{C}^{1 \times N}$ and the channel between U_i and D is denoted as $\mathbf{g}_{u_i d}$. All receiving nodes are inflicted by the additive white Gaussian noise (AWGN) with zero mean and variance σ^2 .

B. Mixed Mobility Model for 3D UAV Movement Process

We consider the multi-parameter MM model [17], [18] which describes the 3D mobility of UAVs in a cylinder of height H and radius R . The MM model is capable of generating wide range of mobility patterns for UAV relays based on specific setting of underlying parameters. In this model, the UAV makes vertical transitions based on RWP mobility model with random dwell time at each waypoint. at time t , the pdf of instantaneous altitude of UAV $h_i(t)$ is given by the weighted sum of a static pdf $f_{h_i}^{st}(x|t)$ and a mobility pdf $f_{h_i}^{mo}(x|t)$ as $f_{h_i}(x|t) = p_s f_{h_i}^{st}(x|t) + (1 - p_s) f_{h_i}^{mo}(x|t)$, where $f_{h_i}^{st}(x|t) = \frac{1}{H}$ and $f_{h_i}^{mo}(x|t) = -\frac{6x^2}{H^3} + \frac{6x}{H^2}$, for $0 \leq x \leq H$, with weight $p_s = \frac{\mathbb{E}[T_s]}{\mathbb{E}[T_s] + \mathbb{E}[T_m]}$ as stay probability at waypoints.

Meanwhile, in the dwell time, the UAV makes RW in horizontal plane by following $z_i(t+1) = z_i(t) + u_i(t)$ with probability p_s , where $z_i(t)$ denotes the projection of UAV's location on ground

plane and $u_i(t)$ is the uniform distribution in ball $B(z_i(t), R')$ with R' as the maximum spatial mobility range. Whereas, it follows $z_i(t+1) = z_i(t)$ with probability $1 - p_s$. Consequently, the pdf of distance $Z_i(t) = \|z_i(t)\|$ is given by $f_{Z_i}(z|t) = \frac{2z}{R^2}$, $0 \leq z \leq R$. Various parameters associated with the MM model are described below: $v_{1,i}(t) \sim [v_{min}, v_{max}]$: Uniformly random velocity of vertical transition at waypoints; $T_s \sim [\tau_{min}, \tau_{max}]$ and $\mathbb{E}[T_s]$: Uniformly random and mean dwell time; T_m and $\mathbb{E}[T_m] = \frac{\ln(v_{max}/v_{min})}{v_{max} - v_{min}} \frac{H}{3}$: Random and mean vertical movement time; and $v_{2,i}(t) = \|z_i(t) - z_i(t-1)\|$ and $\mathbb{E}[v_{2,i}(t)] = \frac{R'}{1.5}$: Random and mean velocity of horizontal transition at waypoints.

C. Channel Models

1) *Satellite Channel*: For channel vector \mathbf{g}_{su_i} whose entries subject to uncorrelated independent and identically distributed (i.i.d.) SR fading, the pdf of $\|\mathbf{g}_{su_i}\|^2$ is given by [5]

$$f_{\|\mathbf{g}_{su_i}\|^2}(x) = \sum_{i_1=0}^{m_{su}-1} \cdots \sum_{i_N=0}^{m_{su}-1} \Xi(N)x^{\gamma-1}e^{-(\beta_u-\delta_u)x}, \quad (1)$$

where $\alpha_u = (2b_{su}m_{su}/(2b_{su}m_{su} + \Omega_{su}))^{m_{su}}/2b_{su}$, $\beta_u = 1/2b_{su}$, and $\delta_u = \Omega_{su}/(2b_{su})(2b_{su}m_{su} + \Omega_{su})$, $\zeta(\kappa) = (-1)^\kappa(1 - m_{su})_\kappa \delta_u^\kappa / (\kappa!)^2$, $(\cdot)_\kappa$ is the Pochhammer symbol [22, p. xliiii], $\Xi(N) = \alpha_u^N \prod_{\kappa=1}^N \zeta(i_\kappa) \prod_{j=1}^{N-1} \mathcal{B}(\sum_{l=1}^j i_l + j, i_{j+1} + 1)$, $\gamma = \sum_{\kappa=1}^N i_\kappa + N$, and $\mathcal{B}(\cdot, \cdot)$ denotes the Beta function [22, eq. 8.384.1]. Further, a free space loss scale factor for satellite links is given as [8] $\sqrt{\mathcal{L}_{su_i}(t)\vartheta_s\vartheta(\theta_{u_i})} = \sqrt{\frac{\vartheta_s\vartheta(\theta_{u_i})}{\mathcal{K}_B\mathcal{T}\mathcal{W}}} \left(\frac{c}{4\pi f_c d_{u_i}(t)} \right)$, where $\mathcal{K}_B = 1.38 \times 10^{-23}$ J/K is the Boltzman constant, \mathcal{T} is the receiver noise temperature, \mathcal{W} is the carrier bandwidth, c is the speed of light, f_c is the carrier frequency, and $d_{u_i}(t)$ is the distance between S and U_i . Here, ϑ_s denotes the antenna gain at satellite, $\vartheta(\theta_{u_i})$ gives the beam gain of satellite towards U_i which can be expressed as $\vartheta(\theta_{u_i}) = \vartheta_{u_i} \left(\frac{\mathcal{J}_1(\rho_{u_i})}{2\rho_{u_i}} + 36 \frac{\mathcal{J}_3(\rho_{u_i})}{\rho_{u_i}^3} \right)$, where θ_{u_i} is the angular separation of U_i from the satellite beam center, ϑ_{u_i} is the antenna gain at U_i , $\mathcal{J}_\varrho(\cdot)$, $\varrho \in \{1, 3\}$ is the Bessel function, and $\rho_{u_i} = 2.07123 \frac{\sin \theta_{u_i}}{\sin \theta_{u_i,3dB}}$ with $\theta_{u_i,3dB}$ as 3dB beamwidth.

2) *UAV Relay-to-Ground Channel*: The terrestrial links between UAV relays U_i and destination D are assumed to follow Nakagami- m fading. Thus, the pdf of the channel gains $|g_{u_i d}|^2$ belongs to gamma distribution

$$f_{|g_{u_i d}|^2}(x) = \left(\frac{m_{ud}}{\Omega_{ud}} \right)^{m_{ud}} \frac{x^{m_{ud}-1}}{\Gamma(m_{ud})} e^{-\frac{m_{ud}x}{\Omega_{ud}}}, \quad (2)$$

where m_{ud} and Ω_{ud} represent an integer-valued fading severity parameter and average channel power, respectively. The instantaneous free-space path loss from UAV U_i to destination D can

be given as $W_{id}^{-\alpha}(t) = (h_i^2(t) + Z_i^2(t))^{-\frac{\alpha}{2}}$, where w_{id} is the distance from U_i to D and α is the path loss exponent.

D. Propagation Model

The satellite S communicates with destination D in two consecutive time phases via variable-gain AF relaying.

In the first phase, at time t , S beamforms its signal $x_s(t)$ (satisfying $\mathbb{E}[|x_s(t)|^2] = 1$) to UAV relay U_i . Thus, the received signal at U_i can be given by

$$y_{u_i}(t) = \sqrt{P_s \mathcal{L}_{su_i}(t) \vartheta_s \vartheta(\theta_{u_i})} \mathbf{g}_{su_i}(t) \mathbf{w}_{su_i}(t) x_s(t) + \nu_{u_i}, \quad (3)$$

where $\mathbf{w}_{su_i}(t) = \frac{\mathbf{g}_{su_i}(t)}{\|\mathbf{g}_{su_i}(t)\|}$ is the beamforming weight vector, ν_{u_i} represents AWGN at D with variance σ^2 .

In the second phase, at time $t+1$, the UAV relay U_i amplifies and forwards the received signal $y_{u_i}(t)$ to destination D with a gain factor $G = \sqrt{\frac{1}{P_s \mathcal{L}_{su_i}(t) \vartheta_s \vartheta(\theta_{u_i}) \|\mathbf{g}_{su_i}(t)\|^2 + \sigma^2}}$. Thus, the received signal at D can be given as

$$y_{id}(t+1) = \sqrt{P_u W_{id}^{-\frac{\alpha}{2}}(t+1)} G y_{u_i}(t) \mathbf{g}_{u_i d} + \nu_d, \quad (4)$$

where ν_d is the AWGN at D with variance σ^2 . From (4), the SNR at D via U_i in the second phase can be calculated as

$$\Lambda_{id}(t+1) = \frac{\Lambda_{su_i}(t) \Lambda_{u_i d}(t+1)}{\Lambda_{su_i}(t) + \Lambda_{u_i d}(t+1) + 1}, \quad (5)$$

where $\Lambda_{su_i}(t) = \frac{P_s \mathcal{L}_{su_i}(t) \vartheta_s \vartheta(\theta_{u_i}) \|\mathbf{g}_{su_i}(t)\|^2}{\sigma^2}$ and $\Lambda_{u_i d}(t+1) = \frac{P_u W_{id}^{-\alpha}(t+1) \|\mathbf{g}_{u_i d}(t+1)\|^2}{\sigma^2}$. Note that since the distance $d_{u_i}(t)$ is very large (e.g., 35,786 Km, for geostationary (GEO) satellite), it is reasonable to assume $d_{u_i}(t) \approx d_u(t)$, $\mathcal{L}_{su_i}(t) \approx \mathcal{L}_{su}(t)$, $\theta_{u_i} \approx \theta_u$, $\rho_{u_i} \approx \rho_u$, and $\vartheta_{u_i} \approx \vartheta_u$, for all i , in this work for subsequent performance analysis.

E. Caching Model and Placement Schemes

Let us consider a catalogue of K content files of equal size C (in the units of number of files) at UAV relays from which the k th file can be requested with popularity defined by the Zipf distribution as $f_k = \left(k^\lambda \sum_{k_1=1}^K k_1^{-\lambda} \right)^{-1}$, where λ denotes the popularity factor. Here, the larger value of λ reflects high popularity files. With limited storage capacity at relays $C \ll K$, a fraction of judiciously chosen files can only be stored, i.e., $MC < K$. As described in [10], [14], we consider the two fundamental yet very popular caching schemes for our HSTN model:

1) *MPC*: If the same content files C are stored at all UAV relays, an arbitrary file with index k can be collaboratively transmitted by a best selected UAV relay according to the criterion $i^*(t) = \arg \max_i \Lambda_{u_{id}}(t), t > 1$.

2) *UC*: If different files are stored at each UAV relay, i.e., the file with index k is stored at $U_i, (i-1)C + 1 \leq k \leq iC$. It maximizes the hit probability of finding the required file.

If the requested file is not cached by the UAV relays, then the conventional opportunistic dual-hop relaying is invoked according to $i^*(t) = \arg \max_i \Lambda_{id}(t), t > 1$. Note that, it may be possible to develop more sophisticated hybrid caching schemes based on a trade-off between MPC and UC schemes which we defer for our future works due to limited space.

For the OP analysis in one snapshot under a causal transmission (i.e., $t > 1$), the time notation is further relaxed.

III. FULLY 3D MOBILE UAV RELAYING

In this section, we conduct OP analysis for fully 3D mobile UAV Relaying with no, MPC, and UC caching schemes.

A. OP with No Caching

With no caching, under i.i.d. SNRs $\Lambda_{id}, \forall i$, the OP of HSTN for a rate \mathcal{R} is given by

$$\begin{aligned} \mathcal{P}_{\text{out}}^{\text{NC}}(\mathcal{R}) &= [\Pr [0.5 \log_2(1 + \Lambda_{id}) < \mathcal{R}]]^M \\ &= [\Psi(\gamma_{\text{th1}})]^M, \end{aligned} \quad (6)$$

where the term $\Psi(\gamma_{\text{th1}})$ is evaluated as

$$\begin{aligned} \Psi(\gamma_{\text{th1}}) &= \Pr [\Lambda_{id} < \gamma_{\text{th1}}] \\ &= 1 - \int_0^\infty \left[1 - F_{\Lambda_{su_i}} \left(\frac{\gamma_{\text{th1}}(x + \gamma_{\text{th1}} + 1)}{x} \right) \right] \\ &\quad \times f_{\Lambda_{u_{id}}}(x + \gamma_{\text{th1}}) dx, \end{aligned} \quad (7)$$

with $\gamma_{\text{th1}} = 2^{2\mathcal{R}} - 1$. In (6), pre-log factor of 0.5 reflects two-slot transmissions. In (7), the cdf $F_{\Lambda_{su_i}}(x)$ can be evaluated using the pdf in (1) for $\Lambda_{su_i} = \eta_s \|\mathbf{g}_{su_i}\|^2$ as

$$\begin{aligned} F_{\Lambda_{su_i}}(x) &= 1 - \sum_{i_1=0}^{m_{su}-1} \cdots \sum_{i_N=0}^{m_{su}-1} \frac{\Xi(N)}{(\eta_s)^\gamma} \sum_{p=0}^{\gamma-1} \frac{(\gamma-1)!}{p!} \\ &\quad \times \Theta_u^{-(\gamma-p)} x^p e^{-\Theta_u x}. \end{aligned} \quad (8)$$

where $\Theta_u = \frac{\beta_u - \delta_u}{\eta_s}$ and $\eta_s = \frac{P_s \mathcal{L}_{su} \vartheta_s \vartheta(\theta_u)}{\sigma^2}$.

Since the mobile UAV relays U_i occupy random locations in 3D space, the distance W_{id} between U_i and D is random. Its pdf for MM model can be expressed using p_s as [18]

$$f_{W_{id}}(w) = p_s f_{W_{id}}^{st}(w) + (1 - p_s) f_{W_{id}}^{mo}(w), \quad (9)$$

where $f_{W_{id}}^{st}(w)$ is the pdf of W_{id} if U_i makes the horizontal transition and $f_{W_{id}}^{mo}(w)$ is the pdf of W_{id} if U_i makes the vertical transition which are expressed, respectively, as

$$f_{W_{id}}^{st}(w) = \begin{cases} \frac{2w^2}{R^2 H}, & \text{for } 0 \leq w < H, \\ \frac{2w}{R^2}, & \text{for } H \leq w < R, \\ \frac{2w}{R^2} - \frac{2w\sqrt{w^2 - R^2}}{R^2 H}, & \\ \quad \text{for } R \leq w \leq \sqrt{R^2 + H^2}, \end{cases} \quad (10)$$

and

$$f_{W_{id}}^{mo}(w) = \begin{cases} \frac{6w^3}{R^2 H^2} - \frac{4w^4}{R^2 H^3}, & \text{for } 0 \leq w < H, \\ \frac{2w}{R^2}, & \text{for } H \leq w < R, \\ \frac{2w}{R^2} - \frac{6w(w^2 - R^2)}{R^2 H^2} + \frac{4w(w^2 - R^2)^{\frac{3}{2}}}{R^2 H^3}, & \\ \quad \text{for } R \leq w \leq \sqrt{R^2 + H^2}. \end{cases} \quad (11)$$

Further, we derive the pdf $f_{\Lambda_{u_i d}}(x) = \frac{d}{dx} F_{\Lambda_{u_i d}}(x)$, where

$$\begin{aligned} F_{\Lambda_{u_i d}}(x) &= \Pr [\eta_u W_{id}^{-\alpha} |g_{u_i d}|^2 < x] \\ &= \int_0^{\sqrt{R^2 + H^2}} \frac{\Upsilon \left(m_{ud}, \frac{m_{ud} x}{\Omega_{ud} \eta_u} r^\alpha \right)}{\Gamma(m_{ud})} f_{W_{id}}(r) dr, \end{aligned} \quad (12)$$

with $\eta_u = \frac{P_u}{\sigma^2}$. After taking a derivative, we can get the pdf

$$\begin{aligned} f_{\Lambda_{u_i d}}(x) &= \frac{1}{\Gamma(m_{ud})} \left(\frac{m_{ud}}{\Omega_{ud} \eta_u} \right)^{m_{ud}} x^{m_{ud} - 1} \\ &\quad \times \int_0^{\sqrt{R^2 + H^2}} r^{m_{ud} \alpha} e^{-\frac{m_{ud} x}{\Omega_{ud} \eta_u} r^\alpha} f_{W_{id}}(r) dr. \end{aligned} \quad (13)$$

Next, we invoke (8) and (13) in (7) and evaluate the result using [22, eq. 3.471.9] to get

$$\begin{aligned} \Psi(\gamma_{\text{th1}}) &= 1 - \sum_{i_1=0}^{m_{su}-1} \cdots \sum_{i_N=0}^{m_{su}-1} \frac{\Xi(N)}{(\eta_s)^\gamma} \sum_{p=0}^{\gamma-1} \frac{(\gamma-1)!}{p!} \\ &\quad \times \sum_{q=0}^p \binom{p}{q} e^{-\Theta_u \gamma_{\text{th1}}} \sum_{n=0}^{m_{ud}-1} \binom{m_{ud}-1}{n} \\ &\quad \times \frac{2}{\Gamma(m_{ud})} \left(\frac{m_{ud}}{\Omega_{ud} \eta_u} \right)^{m_{ud} - \frac{n+q+1}{2}} \Theta_u^{\frac{n+q+1}{2} - (\gamma-p)} \\ &\quad \times \gamma_{\text{th1}}^{m_{ud}+p - \frac{n+q+1}{2}} (\gamma_{\text{th1}} + 1)^{\frac{n+q+1}{2}} \mathcal{J}_1, \end{aligned} \quad (14)$$

where the function \mathcal{J}_1 is given by

$$\begin{aligned} \mathcal{J}_1 &= \int_0^H J_1(r) J_2(r) dr + \int_H^R J_1(r) \frac{2r}{R^2} dr \\ &\quad + \int_R^{\sqrt{R^2+H^2}} J_1(r) J_3(r) dr, \end{aligned} \quad (15)$$

with $J_1(r)$, $J_2(r)$, and $J_3(r)$ as

$$\begin{aligned} J_1(r) &= r^{(m_{ud} - \frac{n+q+1}{2})\alpha} e^{-\frac{m_{ud} \gamma_{\text{th1}} r^\alpha}{\Omega_{ud} \eta_u}} \\ &\quad \times \mathcal{K}_{n-q+1} \left(2 \sqrt{\Theta_u \gamma_{\text{th1}} (\gamma_{\text{th1}} + 1) \frac{m_{ud} \gamma_{\text{th1}} r^\alpha}{\Omega_{ud} \eta_u}} \right), \end{aligned} \quad (16)$$

$$J_2(r) = p_s \frac{2r^2}{R^2 H} + (1 - p_s) \left(\frac{6r^3}{R^2 H^2} - \frac{4r^4}{R^2 H^3} \right), \quad (17)$$

and

$$\begin{aligned} J_3(r) &= p_s \left(\frac{2r}{R^2} - \frac{2r \sqrt{r^2 - R^2}}{R^2 H} \right) \\ &\quad + (1 - p_s) \left(\frac{2r}{R^2} - \frac{6r(r^2 - R^2)}{R^2 H^2} + \frac{4r(r^2 - R^2)^{\frac{3}{2}}}{R^2 H^3} \right), \end{aligned} \quad (18)$$

along with $\mathcal{K}_v(\cdot)$ as the v th order Bessel function of second kind [22]. Note that the derived expression can be readily computed numerically by mathematical softwares.

Asymptotic OP: To gain insights on the achievable diversity order of system, we need to simplify the previous OP expression at high SNR ($P_s, P_u \rightarrow \infty$). At high SNR, we invoke $\Lambda_{id} \leq \min(\Lambda_{su_i}, \Lambda_{u_i d})$ in (7) and neglect the resulting higher-order product of cdfs term to achieve

$$\mathcal{P}_{\text{out}}^{\text{NC}}(\mathcal{R}) \simeq [F_{\Lambda_{su_i}}(\gamma_{\text{th1}}) + F_{\Lambda_{u_i d}}(\gamma_{\text{th1}})]^M. \quad (19)$$

As followed in [5], we can have the simplified cdf $F_{\Lambda_{su_i}}(x)$ under small x as

$$F_{\Lambda_{su_i}}(x) \simeq \frac{\alpha_u^N x^N}{N! \eta_s^N}. \quad (20)$$

Further, by applying the approximation $\Upsilon(v, x) \simeq \frac{x^v}{v}$, for small x , the cdf in (12) can be simplified as

$$F_{\Lambda_{u_i d}}(x) \simeq \frac{1}{m_{ud}!} \left(\frac{m_{ud} x}{\Omega_{ud} \eta_u} \right)^{m_{ud}} \mathcal{J}_2, \quad (21)$$

where \mathcal{J}_2 is

$$\begin{aligned} \mathcal{J}_2 &= \int_0^H r^{m_{ud}\alpha} J_2(r) dr + \int_H^R \frac{2r^{m_{ud}\alpha+1}}{R^2} dr \\ &+ \int_R^{\sqrt{R^2+H^2}} r^{m_{ud}\alpha} J_3(r) dr. \end{aligned} \quad (22)$$

Finally, on substituting the cdf given by (21) into (19), the asymptotic OP can be given by

$$\mathcal{P}_{\text{out}}^{\text{NC}}(\mathcal{R}) \simeq \left[\frac{\alpha_u^N \gamma_{\text{th1}}^N}{N! \eta_s^N} + \frac{1}{m_{ud}!} \left(\frac{m_{ud} \gamma_{\text{th1}}}{\Omega_{ud} \eta_u} \right)^{m_{ud}} \mathcal{J}_2 \right]^M. \quad (23)$$

B. OP with MPC Caching

The OP of considered HSTN with MPC can be given as

$$\mathcal{P}_{\text{out}}^{\text{MPC}}(\mathcal{R}) = \tilde{\mathcal{P}}_{\text{out}}^{\text{MPC}}(\mathcal{R}) \sum_{k=1}^C f_k + \mathcal{P}_{\text{out}}^{\text{NC}}(\mathcal{R}) \sum_{k=C+1}^K f_k, \quad (24)$$

where $\tilde{\mathcal{P}}_{\text{out}}^{\text{MPC}}(\mathcal{R})$ is defined as (for i.i.d. $\Lambda_{u_i d}$)

$$\begin{aligned} \tilde{\mathcal{P}}_{\text{out}}^{\text{MPC}}(\mathcal{R}) &= \Pr \left[\log_2(1 + \max_i \Lambda_{u_i d}) < \mathcal{R} \right] \\ &= [F_{\Lambda_{u_i d}}(\gamma_{\text{th2}})]^M \end{aligned} \quad (25)$$

with $\gamma_{\text{th2}} = 2^{\mathcal{R}} - 1$. In (25), the pre-log factor of one reflects single-hop transmission. Note that in (24), the first term corresponds to the case when D successfully fetches the desired locally cached file at UAV relays. This probability of finding the requested file in local cache at a relay is termed as the hit probability [9]. Whereas, the second term corresponds to the case the desired file is not successfully cached by any relay. This probability of not finding the desired file in local cache is known as the miss probability [9].

Asymptotic OP: Here, at high SNR ($P_s, P_u \rightarrow \infty$), we first simplify the term $\tilde{\mathcal{P}}_{\text{out}}^{\text{MPC}}(\mathcal{R})$ using (21) in (25) as

$$\tilde{\mathcal{P}}_{\text{out}}^{\text{MPC}}(\mathcal{R}) \simeq \left[\frac{1}{m_{ud}!} \left(\frac{m_{ud}\gamma_{\text{th2}}}{\Omega_{ud}\eta_u} \right)^{m_{ud}} \mathcal{J}_2 \right]^M. \quad (26)$$

Then, making use of (19), (26) in (24), the asymptotic OP of MPC can be obtained as

$$\begin{aligned} \mathcal{P}_{\text{out}}^{\text{MPC}}(\mathcal{R}) &\simeq \left[\frac{1}{m_{ud}!} \left(\frac{m_{ud}\gamma_{\text{th2}}}{\Omega_{ud}\eta_u} \right)^{m_{ud}} \mathcal{J}_2 \right]^M \sum_{k=1}^C f_k \\ &+ \left[\frac{\alpha_u^N \gamma_{\text{th1}}^N}{N! \eta_s^N} + \frac{1}{m_{ud}!} \left(\frac{m_{ud}\gamma_{\text{th1}}}{\Omega_{ud}\eta_u} \right)^{m_{ud}} \mathcal{J}_2 \right]^M \sum_{k=MC+1}^K f_k. \end{aligned} \quad (27)$$

C. OP with UC Caching

The OP of considered HSTN with UC can be given as

$$\begin{aligned} \mathcal{P}_{\text{out}}^{\text{UC}}(\mathcal{R}) &= \sum_{i=1}^M \tilde{\mathcal{P}}_{\text{out},i}^{\text{UC}}(\mathcal{R}) \sum_{k=(i-1)C+1}^{iC} f_k \\ &+ \mathcal{P}_{\text{out}}^{\text{NC}}(\mathcal{R}) \sum_{k=MC+1}^K f_k, \end{aligned} \quad (28)$$

where $\tilde{\mathcal{P}}_{\text{out},i}^{\text{UC}}(\mathcal{R})$ is calculated as

$$\tilde{\mathcal{P}}_{\text{out},i}^{\text{UC}}(\mathcal{R}) = \Pr [\log_2(1 + \Lambda_{u_i d}) < \mathcal{R}] = F_{\Lambda_{u_i d}}(\gamma_{\text{th2}}), \quad (29)$$

with $\gamma_{\text{th2}} = 2^{\mathcal{R}} - 1$. Likewise, in (28), the first and second terms represent the hit and miss probabilities, respectively.

Asymptotic OP: The asymptotic OP of UC can be calculated by evaluating (29) using (21) and substituting the result in (28) as

$$\begin{aligned} \mathcal{P}_{\text{out}}^{\text{UC}}(\mathcal{R}) &\simeq \sum_{i=1}^M \frac{1}{m_{ud}!} \left(\frac{m_{ud}\gamma_{\text{th2}}}{\Omega_{ud}\eta_u} \right)^{m_{ud}} \mathcal{J}_2 \sum_{k=(i-1)C+1}^{iC} f_k \\ &+ \left[\frac{\alpha_u^N \gamma_{\text{th1}}^N}{N! \eta_s^N} + \frac{1}{m_{ud}!} \left(\frac{m_{ud}\gamma_{\text{th1}}}{\Omega_{ud}\eta_u} \right)^{m_{ud}} \mathcal{J}_2 \right]^M \sum_{k=MC+1}^K f_k. \end{aligned} \quad (30)$$

IV. FIXED HEIGHT 3D MOBILE UAV RELAYING

In this section, we perform the OP analysis of MPC and UC schemes for another variant of 3D mobile UAV relaying where UAV relays are deployed at a fixed altitude H of the cylindrical region of radius R as shown in Fig. 1. Here, we assume that the UAVs can make transitions in

the circular top of the cylindrical region based on the RW mobility model [15] similar to that described in Section II-B. The resulting steady state distribution of UAV relays remains uniform in the circular disk. For this case, the instantaneous path loss between U_i and D becomes $W_{id}^{-\alpha}(t) = (H^2 + Z_i^2(t))^{-\frac{\alpha}{2}}$, where H is the same for all U_i . Consequent upon the distribution of $Z_i(t)$ as defined in Section II-B, the pdf of W_{id} in one snapshot can be calculated as

$$f_{W_{id}}(w) = \begin{cases} \frac{2w}{R^2}, & \text{for } H \leq w \leq \sqrt{R^2 + H^2}, \\ 0, & \text{else.} \end{cases} \quad (31)$$

A. OP with No Caching

The OP for this case can be computed similar to (6), i.e., $\mathcal{P}_{\text{out}}^{\text{NC}}(\mathcal{R}) = [\Psi(\gamma_{\text{th1}})]^M$. Further, to compute $\Psi(\gamma_{\text{th1}})$ in (7), we first need to find the pdf $f_{\Lambda_{u_i d}}(x)$ based on the pdf $f_{W_{id}}(w)$ as given by (31) in place of (9). Then, utilizing the result in (7), one can obtain

$$\begin{aligned} \Psi(\gamma_{\text{th1}}) &= 1 - \sum_{i_1=0}^{m_{su}-1} \cdots \sum_{i_N=0}^{m_{su}-1} \frac{\Xi(N)}{(\eta_s)^\gamma} \\ &\times \sum_{p=0}^{\gamma-1} \frac{(\gamma-1)!}{p!} \sum_{q=0}^p \binom{p}{q} e^{-\Theta_u \gamma_{\text{th1}}} \sum_{n=0}^{m_{ud}-1} \binom{m_{ud}-1}{n} \\ &\times \frac{2}{\Gamma(m_{ud})} \left(\frac{m_{ud}}{\Omega_{ud} \eta_u} \right)^{m_{ud} - \frac{n+q+1}{2}} \Theta_u^{\frac{n+q+1}{2} - (\gamma-p)} \\ &\times \gamma_{\text{th1}}^{m_{ud}+p - \frac{n+q+1}{2}} (\gamma_{\text{th1}} + 1)^{\frac{n+q+1}{2}} \int_H^{\sqrt{R^2+H^2}} J_1(r) \frac{2r}{R^2} dr. \end{aligned} \quad (32)$$

Asymptotic OP: The asymptotic OP can be calculated based on (19) using the pdf in (31). First, the required asymptotic cdf $F_{\Lambda_{u_i d}}(x)$ can be derived based on (31) as

$$F_{\Lambda_{u_i d}}(x) \simeq \frac{1}{m_{ud}!} \left(\frac{m_{ud} x}{\Omega_{ud} \eta_u} \right)^{m_{ud}} \int_H^{\sqrt{R^2+H^2}} \frac{2r^{m_{ud}\alpha+1}}{R^2} dr. \quad (33)$$

Then, substituting the aforementioned cdf along with the cdf $F_{\Lambda_{su_i}}(x)$ given by (20) into (19), the asymptotic OP for this case can be determined as

$$\mathcal{P}_{\text{out}}^{\text{NC}}(\mathcal{R}) \simeq \left[\frac{\alpha_u^N \gamma_{\text{th1}}^N}{N! \eta_s^N} + \frac{1}{m_{ud}!} \left(\frac{m_{ud} \gamma_{\text{th1}}}{\Omega_{ud} \eta_u} \right)^{m_{ud}} \int_H^{\sqrt{R^2+H^2}} \frac{2r^{m_{ud}\alpha+1}}{R^2} dr \right]^M. \quad (34)$$

B. OP with MPC Caching

The OP of MPC can be similarly evaluated as (24). Here, the term $\mathcal{P}_{\text{out}}^{\text{NC}}(\mathcal{R})$ is the same as evaluated previously in Section IV-A. Further, we calculate $\tilde{\mathcal{P}}_{\text{out}}^{\text{MPC}}(\mathcal{R}) = [F_{\Lambda_{u_i,d}}(\gamma_{\text{th2}})]^M$, where $F_{\Lambda_{u_i,d}}(\gamma_{\text{th2}})$ is obtained by invoking the pdf $f_{W_{id}}(w)$ given by (31) into (12) as

$$F_{\Lambda_{u_i,d}}(x) = \int_H^{\sqrt{R^2+H^2}} \frac{\Upsilon\left(m_{ud}, \frac{m_{ud}x}{\Omega_{ud}\eta_u} r^\alpha\right)}{\Gamma(m_{ud})} \frac{2w}{R^2} dr. \quad (35)$$

Asymptotic OP: Also, the asymptotic OP for this case can be determined by substituting the asymptotic expressions of $\mathcal{P}_{\text{out}}^{\text{NC}}(\mathcal{R})$ and $\tilde{\mathcal{P}}_{\text{out}}^{\text{MPC}}(\mathcal{R})$ in (24). Note that the asymptotic expression of $\mathcal{P}_{\text{out}}^{\text{NC}}(\mathcal{R})$ is already derived as (34). Further, similar to (26), we can derive the asymptotic expression of $\tilde{\mathcal{P}}_{\text{out}}^{\text{MPC}}(\mathcal{R})$ based on the pdf $f_{W_{id}}(w)$ given by (31) as

$$\tilde{\mathcal{P}}_{\text{out}}^{\text{MPC}}(\mathcal{R}) \simeq \left[\frac{1}{m_{ud}!} \left(\frac{m_{ud}\gamma_{\text{th2}}}{\Omega_{ud}\eta_u} \right)^{m_{ud}} \int_H^{\sqrt{R^2+H^2}} \frac{2r^{m_{ud}\alpha+1}}{R^2} dr \right]^M. \quad (36)$$

C. OP with UC Caching

The OP of UC can be similarly evaluated as (28) where $\tilde{\mathcal{P}}_{\text{out},i}^{\text{UC}}(\mathcal{R}) = F_{\Lambda_{u_i,d}}(\gamma_{\text{th2}})$ can be computed using (35). Here, the term $\mathcal{P}_{\text{out}}^{\text{NC}}(\mathcal{R})$ is the same as derived in Section IV-A.

Asymptotic OP: Also, the asymptotic OP for this case can be determined by substituting the asymptotic expressions of $\mathcal{P}_{\text{out}}^{\text{NC}}(\mathcal{R})$ and $\tilde{\mathcal{P}}_{\text{out},i}^{\text{UC}}(\mathcal{R})$ in (28). Note that asymptotic expression of $\mathcal{P}_{\text{out}}^{\text{NC}}(\mathcal{R})$ is already derived as (34). Further, we can derive the asymptotic expression of $\tilde{\mathcal{P}}_{\text{out},i}^{\text{UC}}(\mathcal{R})$ as

$$\tilde{\mathcal{P}}_{\text{out},i}^{\text{UC}}(\mathcal{R}) \simeq \frac{1}{m_{ud}!} \left(\frac{m_{ud}\gamma_{\text{th2}}}{\Omega_{ud}\eta_u} \right)^{m_{ud}} \int_H^{\sqrt{R^2+H^2}} \frac{2r^{m_{ud}\alpha+1}}{R^2} dr. \quad (37)$$

Remark: We first compare the asymptotic OP expressions (23) and (27) corresponding to no caching and MPC caching schemes, respectively, for $\eta_s = \eta_u = \eta$, to reveal their achievable diversity order. The diversity order of the system can be inferred as the minimum exponent of η in the denominator of these asymptotic OP expressions. We found that both $\mathcal{P}_{\text{out}}^{\text{NC}}(\mathcal{R})$ and $\mathcal{P}_{\text{out}}^{\text{MPC}}(\mathcal{R})$ varies proportional to $\frac{1}{\eta^{M \min(N, m_{ud})}}$ at high SNR. This shows that MPC caching scheme can achieve the full diversity order of that of no caching scheme, i.e., $M \min(N, m_{ud})$. However, the MPC caching scheme is expected to offer a relatively higher coding gain over the no caching scheme due to direct single-hop transmission of cached contents. In contrast, the asymptotic OP of UC caching scheme $\mathcal{P}_{\text{out}}^{\text{UC}}(\mathcal{R})$ varies proportional to $\frac{1}{\eta^{\min(MN, m_{ud})}}$ at high SNR. Hence its achievable diversity order is only $\min(MN, m_{ud})$. Note that if $m_{ud} \geq MN$ (e.g., better quality

terrestrial links), both MPC and UC schemes have identical diversity order which depends only on the first-hop satellite links. This reveals that under such conditions UC scheme may achieve both the maximum content diversity and cooperative diversity gains. Intuitively, the content diversity gain of UC scheme is MC which is only C in case of MPC scheme.

V. NUMERICAL RESULTS

For numerical results, based on [8], we set the parameters for satellite as $\mathcal{T} = 300$ K, $\mathcal{W} = 15$ MHz, $c = 3 \times 10^8$ m/s, $d_u = 35,786$ Km, $f_c = 2$ GHz, $\vartheta_u = 4.8$ dB, $\vartheta_s = 53.45$ dB, $\theta_u = 0.8^\circ$, $\theta_{u3dB} = 0.3^\circ$, and $(m_{su}, b_{su}, \Omega_{su}) = (2, 0.063, 0.0005)$ for heavy shadowing. Based on [17]-[20], we set the parameters for UAVs as $v_{1,i} \sim [0.1, 30]$ m/s, $v_{2,i} \sim [0, 40]$ m/s, $H = 80$ m, $R = 100$ m, $\Omega_{ud} = 1$, and $\alpha = 2$. Here, $p_s = 0.5$ is set by adjusting the distribution of T_s . We set $\eta_s = \eta_u = \eta$ as SNR and $\mathcal{R} = 1$. Further, we perform the simulations on Matlab platform for 10^5 independent trials. Before every trial, we initially run all UAV relays independently for 10000 steps based on MM (or RW) model to randomize their locations for fully (or fixed height) 3D mobile UAV relaying.

Figs. 2 and 3 plot the OP curves versus SNR for fully and fixed height 3D mobile UAV relaying, respectively, with no, MPC and UC caching schemes. Apparently, the theoretical, asymptotic, and simulation results are in well agreement with each other. From various curves, we can observe that the MPC caching scheme outperforms significantly the UC and no caching schemes. However, the performance of UC scheme is inferior to the no caching scheme. Firstly, comparing the slopes of curves for $\{M, N, m_{ud}\} = \{2, 2, 1\}$, we observe that the MPC and no caching schemes have a diversity order of 2 while UC caching scheme has a diversity order of 1 (same as no caching with $\{1, 2, 1\}$). This justifies the fact that the UC caching scheme does not achieve the maximum cooperative diversity gain. Similar observations can be made for $\{M, N, m_{ud}\} = \{2, 2, 2\}$ where MPC and UC schemes achieve, respectively, the diversity orders of 4 and 2. Next, we compare the curves for Zipf parameter $\lambda = 0.7$ and 2 in the set $\{M, N, m_{ud}\} = \{2, 2, 2\}$. Herein, we find that as λ increases from 0.7 to 2, the relative performance gain of MPC caching scheme is quite larger as compared to that of the UC caching scheme. However, the UC scheme offers the largest content diversity benefits over its MPC counterpart. Finally, on comparing the set of OP curves of Figs. 2 and 3, we conclude that the performance of cache-enabled fully 3D mobile UAV relaying is remarkably better than that of fixed height one due to lower mean distance between UAV and UE.

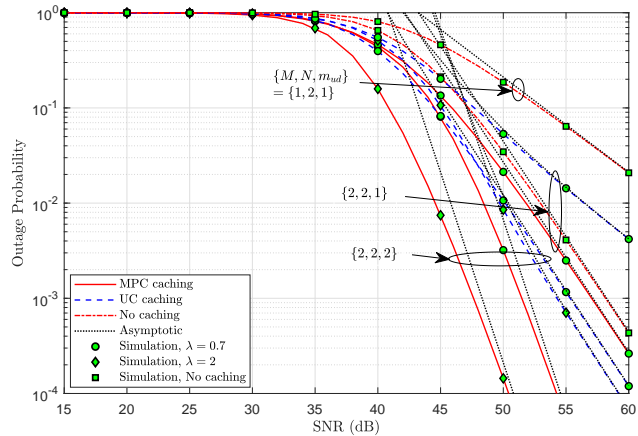


Fig. 2: OP of fully 3D mobile UAV relaying versus SNR.

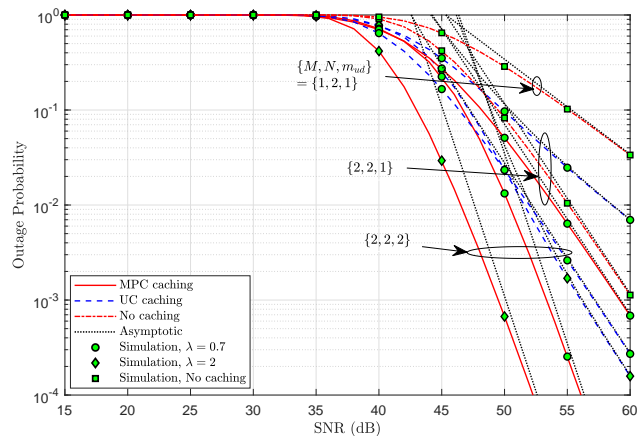


Fig. 3: OP of fixed height 3D mobile UAV relaying versus SNR.

VI. CONCLUSION

We have evaluated the OP of an HSTN which comprises of a multiantenna satellite, a ground UE and multiple cache-enabled AF 3D mobile UAV relays. We considered the fundamental MPC and UC caching schemes at UAV relays. In addition, we considered the fully and fixed altitude 3D mobile UAV relaying for outage performance analysis. We have the following observations: (a) MPC dominates both UC and no caching schemes; (b) fully 3D mobile UAV relaying achieves better performance gains over the fixed height one.

REFERENCES

- [1] G. Giambene, S. Kota, and P. Pillai, "Satellite-5G integration: A network perspective," *IEEE Netw.*, vol. 32, no. 5, pp. 25-31, Sep./Oct. 2018.
- [2] A. Guidotti et al., "Architectures and key technical challenges for 5G systems incorporating satellites," *IEEE Trans. Veh. Technol.*, vol. 68, no. 3, pp. 2624-2639, Mar. 2019.
- [3] M. R. Bhatnagar and Arti M. K., "Performance analysis of AF based hybrid satellite-terrestrial cooperative network over generalized fading channels," *IEEE Commun. Lett.*, vol. 17, no. 10, pp. 1912-1915, Oct. 2013.
- [4] K. An, M. Lin, and T. Liang "On the performance of multiuser hybrid satellite-terrestrial relay networks with opportunistic scheduling," *IEEE Commun. Lett.*, vol. 19, no. 10, pp. 1722-1725, Oct. 2015.
- [5] P. K. Upadhyay and P. K. Sharma, "Max-max user-relay selection scheme in multiuser and multirelay hybrid satellite-terrestrial relay systems," *IEEE Commun. Lett.*, vol. 20, no. 2, pp. 268-271, Feb. 2016.
- [6] S. Sreng, B. Escrig, M.-L. Boucheret, "Exact symbol error probability of hybrid/integrated satellite-terrestrial cooperative network," *IEEE Trans. Wireless Commun.*, vol. 12, no. 3, pp. 1310-1319, Mar. 2013.
- [7] P. K. Sharma, P. K. Upadhyay, D. B. da Costa, P. S. Bithas, and A. G. Kanatas, "Performance analysis of overlay spectrum sharing in hybrid satellite-terrestrial systems with secondary network selection," *IEEE Trans. Wireless Commun.*, vol. 16, no. 10, pp. 6586-6601, Oct. 2017.
- [8] K. Guo, K. An, B. Zhang, Y. Huang, and G. Zheng, "Outage analysis of cognitive hybrid satellite-terrestrial networks with hardware impairments and multi-primary user," *IEEE Wireless Commun. Lett.*, vol. 7, no. 5, pp. 816-819, Apr. 2018.
- [9] Z. Chen, J. Lee, T. Q. S. Quek, and M. Kountouris, "Cooperative caching and transmission design in cluster-centric small cell networks," *IEEE Trans. Wireless Commun.*, vol. 16, no. 5, pp. 3401-3415, May 2017.
- [10] C. Psomas, G. Zheng, and I. Krikidis, "Cooperative wireless edge caching with relay selection," in *Proc. IEEE ICC.*, Paris, France, May 2017.
- [11] L. Fan, N. Zhao, X. Lei, Q. Chen, N. Yang, and G. K. Karagiannidis, "Outage probability and optimal cache placement for multiple amplify-and-forward relay networks," *IEEE Trans. Veh. Technol.*, vol. 67, no. 12, pp. 12373-12378, Dec. 2018.
- [12] A. Kalantari, M. Fittipaldi, S. Chatzinotas, T. X. Vu, and B. Ottersten, "Cache-assisted hybrid satellite-terrestrial backhauling for 5G cellular networks," in *Proc. IEEE Globecom*, Singapore, Dec. 2017.
- [13] T. X. Vu, N. Maturo, S. Vuppala, S. Chatzinotas, J. Grotz, and N. Alagha, "Efficient 5G edge caching over satellite," in *Proc. ICSSC*, Niagara Falls, ON, Canada, Aug. 2018.
- [14] K. An, Y. Li, X. Yan, and T. Liang, "On the performance of cache-enabled hybrid satellite-terrestrial relay networks," *IEEE Wireless Commun. Lett.*, vol. 8, no. 5, pp. 1506-1509, Feb. 2019.
- [15] M. Banagar and H. S. Dhillon, "Performance characterization of canonical mobility models in drone cellular networks," *IEEE Trans. Wireless Commun.*, vol. 19, no. 7, pp. 4994-5009, July 2020.
- [16] M. N. Anjum and H. Wang, "Mobility modeling and stochastic property analysis of airborne network," *IEEE Trans. Netw. Sci. Eng.*, vol. 7, no. 3, pp. 1282-1294, July-Sept. 2020.
- [17] P. K. Sharma and D. I. Kim, "Coverage probability of 3-D mobile UAV networks," *IEEE Wireless Commun. Lett.*, vol. 8, no. 1, pp. 97-100, Feb. 2019.
- [18] P. K. Sharma and D. I. Kim, "Random 3D mobile UAV networks: Mobility modeling and coverage probability," *IEEE Trans. Wireless Commun.*, vol. 18, no. 5, pp. 2527-2538, May 2019.
- [19] P. K. Sharma, D. Deepthi, and D. I. Kim, "Outage probability of 3-D mobile UAV relaying for hybrid satellite-terrestrial networks," *IEEE Commun. Lett.*, vol. 24, no. 2, pp. 418-422, Feb. 2020.

- [20] P. K. Sharma and D. I. Kim, "Secure 3D mobile UAV relaying for hybrid satellite-terrestrial networks," *IEEE Trans. Wireless Commun.*, vol. 19, no. 4, pp. 2770-2784, Apr. 2020.
- [21] P. K. Sharma, D. Gupta, and D. I. Kim, "Cooperative AF-based 3D mobile UAV relaying for hybrid satellite-terrestrial networks," in *Proc. IEEE VTC-Spring*, Antwerp, Belgium, May 2020.
- [22] I. S. Gradshteyn and I. M. Ryzhik, *Tables of Integrals, Series and Products*, 6th ed. New York: Academic Press, 2000.